AIAA'85

AIAA-85-0559

The Control of Transitional Flows

P.J. Strykowski and K.R. Sreenivasan
Yale University, New Haven, CT.

AIAA Shear Flow Control Conference

March 12-14, 1985/Boulder, Colorado

THE CONTROL OF TRANSITIONAL FLOWS

P.J. Strykowski* and K.R. Sreenivasan†
Mason Laboratory, Yale University, New Haven, CT 06520

Abstract

Primary to any control of transitional flows is the consideration of the basic state and the disturbance. One of our objectives is to actively suppress the disturbance so that stability is restored to the basic state. Another objective is to alter locally the characteristics of the basic state at the inception of instability and prevent or postpone further evolution of the flow towards turbulence. Work is in progress along both lines; samples of this work are briefly reported here.

The paper is in two parts. In part I, our interest is in forcing an instability in a Blasius boundary layer, and in manipulating the instability by superimposing another disturbance of controllable phase. This is in the spirit of the previous work by Milling [1], Liepmann et al.,[2], and Thomas[3], but is different in detail. In part II, we are interested in establishing the principle that an absolutely unstable flow can be rendered stable by a suitable local manipulation of the basic state. The example we have studied here is the suppression of vortex shedding behind circular cylinders. At the time of this writing, our success in the former case is limited to situations before the onset of strong three-dimensionalities; in the latter, it is restricted to fairly low Reynolds numbers.

Part I

Introduction

It can be shown from first principles[4] that the energy of a linear disturbance can be depleted if a fluctuating body force (produced for example by periodically oscillating a ribbon in the streamwise direction) or fluctuating mass addition can be introduced into the flow at a properly chosen phase with respect to the disturbance. This assertion is true for nonlinear disturbances also – this too can be shown from first principles[4,5] – with the extra provision that the fluctuating body force and mass are to be interpreted as 'effective', that is, as including contributions from the basic velocity distribution and the fluctuations themselves. Our interest is in using these ideas for transition control, in the linear, nonlinear and aperiodic stages.

In a companion paper[6], we have shown how pressure oscillations of large amplitude can be actively controlled in a variety of circumstances.

Controlled Tollmien-Schlichting (T-S) Waves

The most proper procedure for the suppression of a naturally created T-S is the use of a signal of equal magnitude and opposite phase, produced by active feedback. The first step in this procedure involves the suppression of the T-S waves created in a controlled manner. In the past, controlled T-S waves have been produced in laminar boundary layers by various means; vibrating wires[1], use of Ohmic heating elements[2], vibrating ribbons[3], and acoustic excitation[7]. Liepmann, Brown and Nosenchuck[2] used wall-imbedded heating elements in water boundary layers to produce controlled T-S waves and eliminate them by wave cancellation. Liepmann and Nosenchuck[8] also successfully used active control techniques. The extension of their technique to boundary layers in air is not obvious because of the differences in the conductive and diffusive properties between air and water. The first aspect of the present study was to examine whether the heating element technique could be used in air to produce (and suppress) the T-S waves.

The experimental setup consisted of a low turbulence wind tunnel ($u_{rms}/U_\infty \leq 0.03\%$, u_{rms} being the *rms* magnitude of the streamwise velocity fluctuations, and U_∞ being the freestream velocity). The tunnel was supplied with compressed air stored in two large storage tanks. Air entered two settling chambers packed with damping material, downstream of which were two contractions and several carefully placed screens; see Fig.1. The settling chambers were acoustically lined and the total combination of experi-

* Graduate student.
† Associate Professor, member AIAA.

mental apparatus permitted no discrete frequencies in the freestream spectral density distribution. Downstream of the second contraction we placed a test section 30.5 cm wide and 1.27 cm deep. The rather small cross section was necessary to accommodate volume flow restrictions of our compressor. The test section was 46 cm long and was carefully diverged to produce constant pressure over the region of measurement. For all conditions of measurement in the region of interest, the depth of the test section was greater than approximately 3δ where δ is the boundary layer thickness. A typical boundary layer profile can be seen in Fig.2.

For the experiments with the heating element, T-S waves were designed to occur at a freestream velocity near 6 m/sec and $Re_x \simeq 1.2 \times 10^5$. Because resistive heating is proportioned to the square of the applied current, the oscillation produced by heating will be twice the frequency of the input signal. Therefore the driving signal frequency was set to one-half the desired T-S wave frequency ($f_{TS} \approx 75Hz$).

Liepmann et al.[2] pointed out that the effect of the heating element can be interpreted in two ways. By virtue of changes in viscosity associated with temperature changes, one can interpret the heating element to produce a fluctuating body force. Alternatively, a periodically heated wall-element also can be imagined to produce a fluctuating normal velocity. Simple estimates suggest that the latter is likely to be the more dominant one. Liepmann et al. estimated this magnitude in water to be

$$| v\prime/U\infty |\sim 0.0003\Delta T,$$

where ΔT is the temperature rise in $\deg C$, and pointed out that it will be 20 times smaller in air. For the conditions of their experiment which produced T-S waves, Liepmann et al. estimated a ΔT of about $3\deg C$. To produce similar effects in air, it follows that a larger ΔT (of the order of $60\deg C$) will probably be required.

Heating the flush-mounted heating element to this degree, however, did not produce the T-S waves. In fact, even higher amounts of heating (estimated surface temperature $450°C$) did not produce them. We suspect that the substantial d.c. heating associated with the periodic resistive heating will alter the mean velocity distribution enough, so that one is no longer dealing with a Blasius profile. Mean velocity data taken approximately 2.5δ downstream of the heater (Fig.3) clearly shows that large amounts of heating cause substantial distortion in the profile. The power input to the heating element was approximately 2 Watts/cm (enough to produce a pale red color).

The power delivered to the heating element is used up partly in increasing the entropy of the gas, and partly in setting up a velocity perturbation. Clearly, the fact that we do not see any velocity perturbations of the periodic nature in the experiment described above must mean that the latter fraction must be small in the case of air. To examine whether this will be different if the heating element is located off the wall, a fine steel wire (d=0.13 mm) was mounted at various locations off the surface, both inside and outside the boundary layer. (We note that this actually defeats our purpose of producing T-S waves by non-intrusive methods, but the diversion seemed worthwhile.) Large amplitude T-S waves were easily produced, although, closer observation revealed that physical vibration of the wire, at twice the driving frequency, was the cause of the disturbance. (The wire itself shed no vortices.) When the physical excitation was eliminated it became clear that T-S waves could not be produced by the off-surface heating either.

Again, it appears to us that the substantial distortion produced in the mean velocity profile appears to inhibit the development of T-S waves. Figure 4 shows mean velocity data taken 5δ downstream of the off-surface heating element. As before, the heating has distorted the velocity profile. Calculation of the shape factor H (where $H = \delta*/\theta, \delta*$ is the displacement thickness and θ is the momentum thickness) of the two distorted profiles in Figs.3 and 4 provides values of 2.92 and 2.72 for the wall-mounted respectively; this can be compared to a theoretical value H=2.59 appropriate to a Blasius profile. It should be pointed out that the low Reynolds number of the flow does not permit premature transition to turbulence, even though the profile is highly distorted. Further, order of magnitude calculations suggest that buoyancy effects do not contribute significantly to the flow dynamics.

As pointed out above, the most important effect of a heating element is equivalent to producing small amounts of periodic suction and blowing. Since the heating element method of non-intrusively producing T-S waves failed, it appeared desirable that direct suction and blowing be tried. By this means, we have successfully

produced the classical T-S waves; we have also cancelled them by antiphase superposition. This will be discussed in the next section.

To avoid any net mass addition during periodic suction and blowing we chose to vibrate a wire in a slot as shown in Fig.5. Alternating current is passed through the wire in the presence of a magnetic field; the vibration of the wire will periodically move mass into and out of the boundary layer. Copper wire was used to minimize the Ohmic heating and the wire was longer than the test section width for better two-dimensionality of the oscillation.

The disturbance created by the suction-blowing slot was compared with theoretical data on T-S waves; the wave was produced at a T-S wave frequency of 97 Hz. The eigenfunction and phase of the disturbance were measured approximately 5δ downstream of the slot; these show reasonable agreement with theory (Figs. 6 and 7). Notice that agreement between the experiment and theory would not be exact since the experimental data were taken at $R_\delta* = 690$ and the theory[9] corresponds to an $R_\delta*$ of 770. Also, no computed phase information was available near $R_\delta*$ of 690 so the curve shown is simply the best fit to the data. Figure 8 shows the approximate exponential growth of the T-S wave after an initial adjustment discussed below.

Careful consideration was given to ascertain whether the T-S waves were actually the result of periodic mass fluctuations or of the acoustic wave possibly set up by the vibrating wire. Simple tests suggest that the acoustic disturbance was attenuated strongly, and that periodic mass injection/suction was indeed responsible for the wave. It appears useful to document the evolution of the T-S wave from the suction/injection slot. Immediately above the downstream edge of the slot, two types of disturbances were commonly produced; the oscillograms in Fig.9 show the hot wire signals and the slot arrangements used to produce them. Under the conditions described in the upper trace of Fig.9, the suction/blowing slot works as it was supposed to, producing a disturbance at the driving frequency. If the wire fits too tightly in the slot, wire oscillation will be inhibited and no T-S wave will be produced. When the adjustable slot is widened slightly, air is allowed to pass between the wire and the slot wall, in the direction opposite to the moving wire. This arrangement produces a disturbance containing predominantly the driving frequency, but with a superimposed frequency of twice the value. It usually requires some manipulation to obtain the optimal conditions of operation; however, slightly downstream of the slot, both techniques were equally able to produce T-S waves at the driving frequency. Note that for the conditions of our experiment, twice the driving frequency lies well outside the region of instability and is quickly damped out. In Fig.10a, the amplitudes of the streamwise fluctuations caused by the slot are plotted for various normal distances from the plate. Oscillograms corresponding to points (a)-(e) on Fig.10a are displayed in Fig.10b. Several comments should be made about the initial stages of the disturbance. At small distances above the slot (say $y/\delta \sim 0.2$) we see a small amplitude oscillation at the driving frequency similar to trace (a) in Fig.9. As we move downstream at this fixed y/δ, the amplitude grows rapidly [trace (a) Fig.10b] and soon thereafter reaches a minimum [trace (b)]. Further downstream the amplitude gain increases. This "start up" phase of the disturbance, which occurs within 1-2 δ downstream of the slot, can be explained as follows: during a positive displacement of the wire, a small jet emerges from the slot carrying an upward momentum; this jet soon reattaches onto the wall some distance downstream of the slot. The minimum occurring in the amplitude of the disturbance, as well as trace (b) in Fig.10b, correspond to the position upstream of the reattaching jet. Downstream, the signal picks up and develops as demanded by the dynamics of the flow.

It is clear that the physical picture of the momentum jet implies that, above the penetration distance of the jet, the fluctuations produced should display no minimum, and this is borne out by the uppermost curve in Fig.10a, and the signals (e) and (f) in Fig.10b. The estimated peak to peak velocity fluctuation introduced into the boundary layer is of the order of 0.10% of the freestream velocity.

A comment appears necessary regarding the kink in the phase diagram of Fig.7. The reason for the kink is unclear, but it may be related to the upstream slot history. In a preliminary effort to eliminate the kink by restoring the proper boundary conditions at the slot, a very thin tape was placed over the slot. We had hoped that the oscillation in the slot would be transmitted into small amplitude vibrations of the tape and hence excite the desired T-S waves. At this time

we have had no success with this technique, but efforts are continuing in that direction.

Cancellation and Amplification of T-S Waves by Periodic Suction and Blowing

Since we have shown that T-S waves can be created by suction and blowing, we would like to cancel controlled T-S waves by this technique. A T-S wave was created at location (1) on the stability diagram of Fig.11; this is the T-S wave that we would like either to suppress or amplify by generating another properly phased T-S wave at station (2). The flow was monitored at station (3) and downstream up to the end of the test section. All oscillograms to be given in Fig.12, except trace (a), were obtained at station (3). The same driving signal (frequency=97Hz) was used to produce both waves; the signal to the downstream wire was first passed through a circuit which allowed the phase of the output to be varied continuously with respect to the input. Notice that we selected station (2) to be on branch II of the stability diagram.

Trace (a) in Fig.12 is the background disturbance; this trace was taken at station (1). Trace (b) is a typical T-S wave generated at station (1). Careful selection of the phase and amplitude of the T-S wave generated at station (2) will determine the reinforcement [trace (c)], or cancellation [trace (d)]. The driving signals used to generate the two T-S waves during reinforcement and cancellation are shown in traces (e) and (f), respectively. Notice that the phase relationships seen in oscillograms (e) and (f) are not the true phase relationships between the interacting T-S waves, but are modified by the differences in convection distances for the two T-S waves.

Conclusions

We have shown that:

(a) The heating element technique successfully employed by Liepmann et al.[2] to produce T-S waves in water boundary layers does not appear to be appropriate for air.

(b) Periodic suction and injection can be used to produce T-S waves without much interference of the basic state.

(c) These T-S waves can be cancelled much in the same spirit as the previous work of References 1-4.

Further work in progress is aimed towards controlling three-dimensional and aperiodic fluctuations.

Part II

Introduction

As stated earlier, we would like to globally stabilize an absolutely unstable flow by locally altering the basic state of the flow. We choose to suppress vortex shedding behind circular cylinders at low Reynolds numbers. In attempting this, we manipulate the basic state whose instability normally develops downstream into a saturated new state. In contrast to the study in Part I, we do not control the disturbance after it is generated, but stabilize the basic state in such a way that disturbances which would normally have appeared and grown do not appear forever.

The Phenomenon

Consider a nominally two-dimensional flow past a circular cylinder. A hydrogen bubble visualization of the vortex shedding behind the cylinder, the phenomenon known at least since the days of Leonardo da Vinci and experimentally studied since the days of Strouhal, is shown in Fig.13; the Reynolds number Re, based on the cylinder diameter D and the upstream flow speed U, is about 80.

Let us now introduce another parallel cylinder of diameter d (greater than about D/20) somewhat downstream and to one side of the vortex shedding cylinder (see Fig.14). The hydrogen bubble visualization (Fig.15a) shows clearly that the vortex shedding is completely suppressed; Re is about 80. Hot-wire traces (Fig.15b) confirm this conclusion.

For $40 \leq Re \leq 80$, there is a finite region (called the region of suppression) within which the placement of the thinner (or the control) cylinder can achieve total suppression. Figure 16 shows the regions of suppression for three values of the diameter ratio, D/d; clearly, the region of suppression is reduced with increasing D/d. If one decreases the diameter ratio D/d, complete suppression at Reynolds numbers marginally higher than 80 (say 90) appears possible.

Interestingly, mildly heating (in air flow) the control cylinder with direct current dramatically widens the region of suppression (Fig.17, for D/d $\simeq$ 15); again the suppression is as complete as typified by Fig.15b. Notice that with heating the control cylinder does not have to be confined to regions close to one of the shear layers for effecting control. Increasing the amount of heating widens the region of suppression.

At higher Reynolds numbers, say 120, and for diameter ratios of the order of 10, and the control cylinder cold, vortex shedding can be suppressed completely only for x/D $\simeq$ 5 but not beyond. We should emphasize that even in this case, the influence of the control cylinder pervades in a nontrivial way for streamwise distances of the order of 100 D. However, by heating the control cylinder, one can again find regions of total suppression (Fig.18). At a fixed Re, these regions again widen with increase in heating; furthermore, the control becomes effective at lower heating rates of the control cylinder when it is in the shear layer than when it is in the center plane or vicinity.

Further Results

One manifestation of global suppression of vortex shedding is the concentration (compare Figs.13 and 15a) of the bulk of momentum defect to a narrower region than is normally the case in the presence of shedding, and correspondingly enhance the maximum momentum defect. Figure 19 shows, at x/D = 58, mean velocity profiles with and without control.

Repeated measurements have shown that the modified momentum defect behind the cylinder results in a net drag reduction above and beyond the increase owing to the presence in the stream of the control cylinder. It should be emphasized (see Fig.19) that the velocity defect in the controlled case occurs close to the cylinder axis, and is accompanied by a weak overshoot spread over a large width. This latter fact is especially important for a proper measurement of drag. Typically, for Re = 80, there is about a 20% reduction in the drag coefficient.

Discussion and Conclusion

The explanation for these (and other) observed phenomena appears to be related to the subtle changes in the flow details close to the vortex shedding cylinder that are brought about by the presence of the control cylinder. This can be seen clearly by a comparison of Fig.20 (which to the usual vortex shedding case) with Figs.21 and 22 corresponding to complete suppression; the Reynolds number in all these figures is about 90 and D/d $\simeq$ 7. Note that the control cylinder in each of the figures, 21 and 22, has the effect of diverting part of the fluid into the wake from outside, but the detailed conditions (such as the position of the control cylinder) are different from one figure to another.

The complete explanation for the phenomenon discussed here must obviously await further work. It is natural to expect that the stability calculations based on mean velocity distributions near the cylinder would be of some help. These are currently being contemplated but two comments should be made.

The first comment to be made is that the effect of the control cylinder appears to be the establishment of conditions effectively similar to those existing at a lower Reynolds number. The evidence for this is somewhat indirect. In an earlier study[10], we showed that transition to turbulence in wakes behind circular cylinders is not a continuous sequence of bifurcations leading to states of increasing complexity but is a sequence of events alternating between 'chaos' and 'order'. One simple way of distinguishing these alternations between the states of chaos and order is to examine with fine resolution the power spectra of the (streamwise) velocity fluctuation. Within windows of chaos, loosely speaking, the power spectra will have a large broadband component while they are composed of discrete modes (one or several) in regions of order. Figure 23 summarizes the situation.

Suppose now that we stationed ourselves in the window of order called 'three frequency quasiperiodicity', and hold the Reynolds number fixed (say, around 80). Suppose now that we introduce the control cylinder and move it gradually closer and closer to the cylinder, and examine the characteristics of the velocity fluctuations measured at the location shown in the inset of Fig.23. We observe that the character of the velocity signal at the fixed x/D and this fixed Reynolds number can be altered so as to shift it to some window of order of chaos situated to the left of where we are stationed. For each position of the control cylinder, there corresponds a par-

ticular state. Eventually, for some position of the control cylinder, the shedding completely disappears. In our view, these observations suggest that the velocity field near (but not too near) the cylinder is altered by the control cylinder so as to correspond to an equivalent low Reynolds number state.

The second comment to be made, also speculative, is related to how the control cylinder causes a possible change in the nature of instability of the near field flow. If we rely on Koch's work[11] , it appears that the normal wake is absolutely unstable[12] and a resonance mechanism determines the vortex shedding frequency. Our speculation is that a cold control cylinder on one side of the vortex shedding cylinder generates sufficient asymmetry of the near wake, so that the entire wake becomes convectively unstable, and the resonance is eliminated.

We close our discussion with the comment that the control cylinder does not always have the effect of suppressing the vortex shedding. A suitable position for it can in fact be found such that the flow visualization of Fig.24 results.

Acknowledgements

This work was supported by a grant from the AFOSR. We have benefitted from our discussions with Professors B.T. Chu, P.A. Monkewitz and H. Oertel.

References

1. Milling, R.W.: Tollmien-Schlichting Wave Cancellation. Physics of Fluids, Vol.24, 1981, pp.979-981.

2. Liepmann, H.W.; Brown, G.L.; and Nosenchuck, D.M.: Control of Laminar-Instability Waves Using a New Technique. Journal of Fluid Mechanics, vol. 118, 1982, pp. 187-200.

3. Thomas, A.S.W.: The Control of Boundary-Layer Transition Using a Wave-Superposition Principle. Journal of Fluid Mechanics, vol. 137, 1983, pp. 233-250.

4. Chu, B.T.: On the Energy Transfer to Small Disturbances in Fluid Flow. Acta Mechanica, vol. 1, 1965, pp. 215-234.

5. Sreenivasan, K.R.; Laurien, E.; and Kleiser, L.: Numerical Investigation of Active Transition Control: A Progress Report. Under preparation.

6. Sreenivasan, K.R.; Raghu, S.; and Chu, B.T.: The Control of Pressure Oscillations in Combustion and Fluid Dynamical Systems. AIAA Shear Flow Control Conference, Boulder, Colorado, March 12-14, 1985, Paper 85-0540.

7. Gedney, C.J.: The Cancellation of a Sound-Excited Tollmien-Schlichting Wave with Plate Vibration. Physics of Fluids, vol. 26, May 1983, pp. 1158-1160.

8. Liepmann, H.W.; and Nosenchuck, D.M.: Active Control of Laminar-Turbulent Transition. Journal of Fluid Mechanics, vol. 118, 1982, pp. 201-204.

9. Ross, J.A.; Barnes, F.H.; Burns, J.G.; and Ross, M.A.S.: The Flat Plate Boundary Layer. Part 3. Comparison of Theory with Experiment. Journal of Fluid Mechanics, vol. 43, Part 4, 1970, pp. 819-832.

10. Sreenivasan, K.R.: Transition to Turbulence in Fluid Flows and Low-Dimensional Chaos. To appear in Fundamentals of Fluid Mechanics (eds. S.H. Davis and J.L. Lumley), Springer-Verlag, 1984.

11. Koch, W.: Local Instability Characteristics and Frequency Determination of Self-Excited Wake Flows. To appear in Journal of Sound and Vibration, 1985.

12. Huerre, P.; Monkewitz, P.A.: Absolute and Convective Instabilities in Free Shear Flows. Submitted to Journal of Fluid Mechanics, 1985.

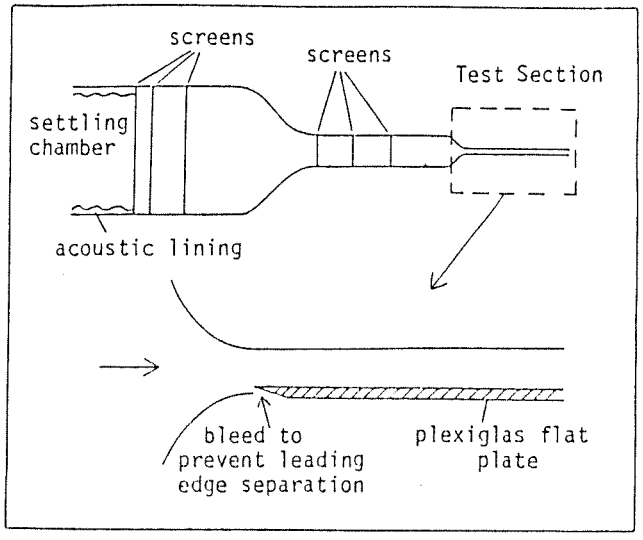

Fig. 1. Schematic of the low turbulence wind tunnel and a detailed view of the test section.

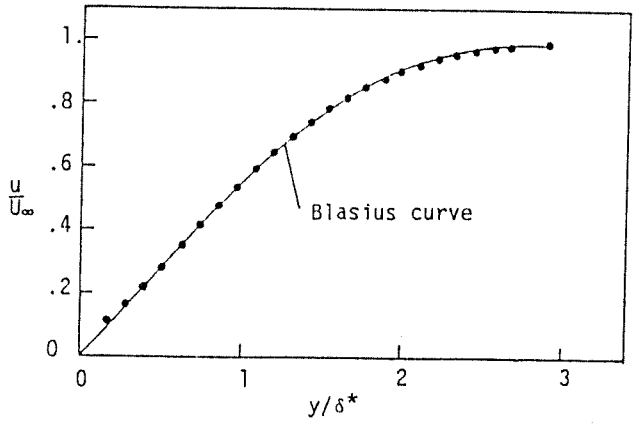

Fig. 2. Comparison of a measured laminar profile with theory; $U_\infty \approx 6$ m/sec and $R_{\delta^*} \approx 450$.

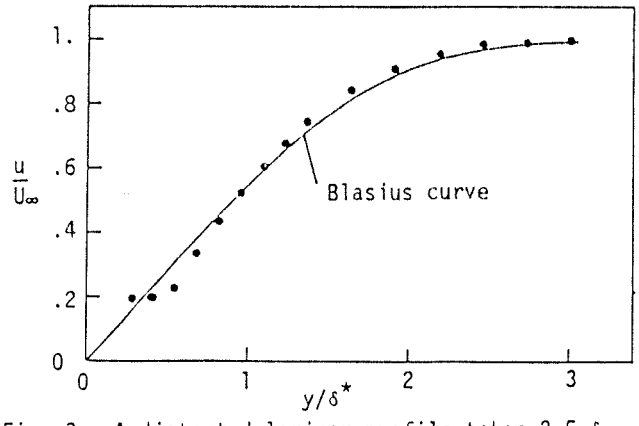

Fig. 3. A distorted laminar profile taken 2.5 δ downstream of a wall-mounted heating element; $U_\infty \approx 6$ m/sec and $R_{\delta^*} \approx 770$. The estimated temperature of the heating element is 450 °C. (Power input is 2 watts/cm.)

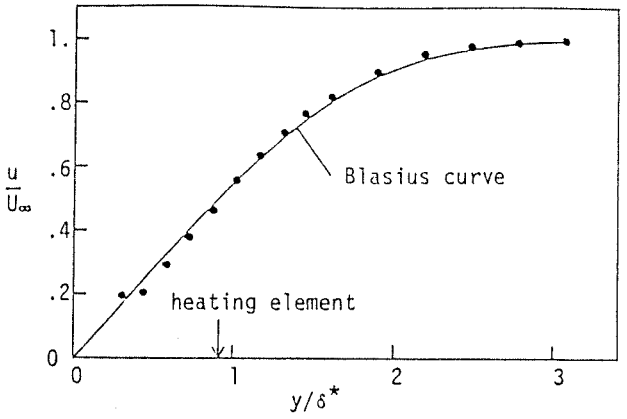

Fig. 4. A distorted profile taken 5δ downstream of an off-surface heating element. The heating element was positioned at $y/\delta^* \approx 0.9$; $U_\infty \approx 6$ m/sec and $R_{\delta^*} \approx 690$.

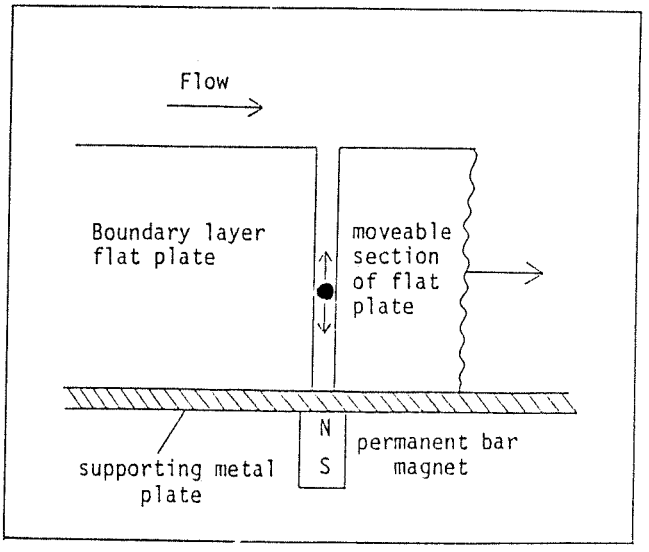

Fig. 5. Schematic of device used to produce periodic suction and blowing. Copper wire (d=.18mm) was oscillated in the snug-fitting slot.

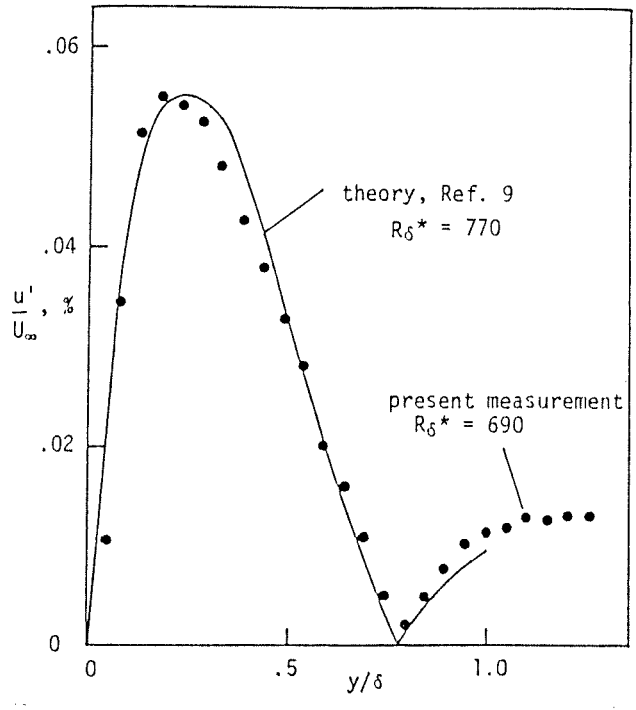

Fig. 6. Comparison of eigenfunction between the present data (U_∞ = 6 m/sec) and theory. The amplitudes were normalized by integrating from y/δ of 0 to 1.

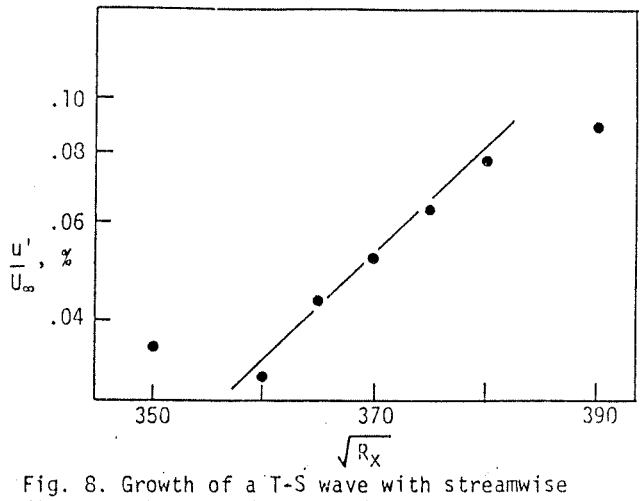

Fig. 8. Growth of a T-S wave with streamwise distance. U_∞ = 6 m/sec and f = 85 hz.

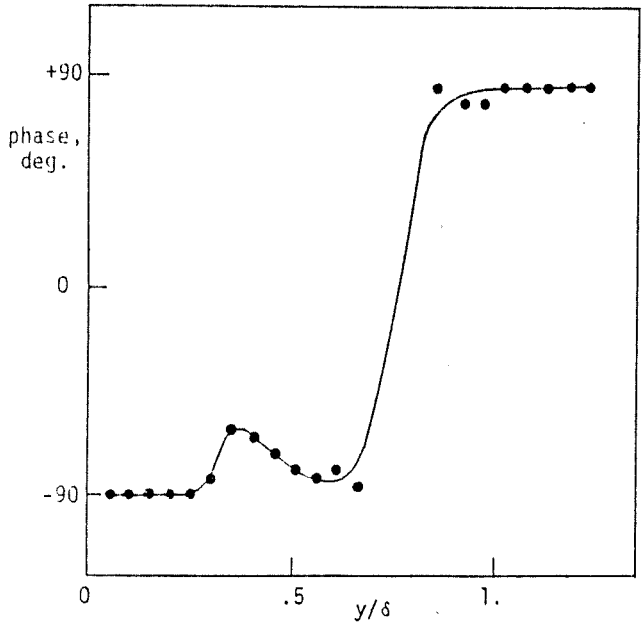

Fig. 7. Relative phase of the T-S wave. The solid curve represents the best fit to the data; U_∞ = 6 m/sec and R_δ^* = 690.

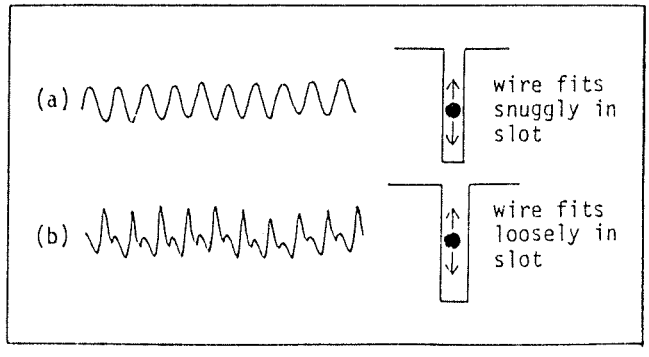

Fig. 9. Signals produced by the suction-blowing slot. Oscillograms taken immediately above slot at y/δ^* = 0.3. Notice that when the fit is loose, the harmonic is superposed on the driving frequency.

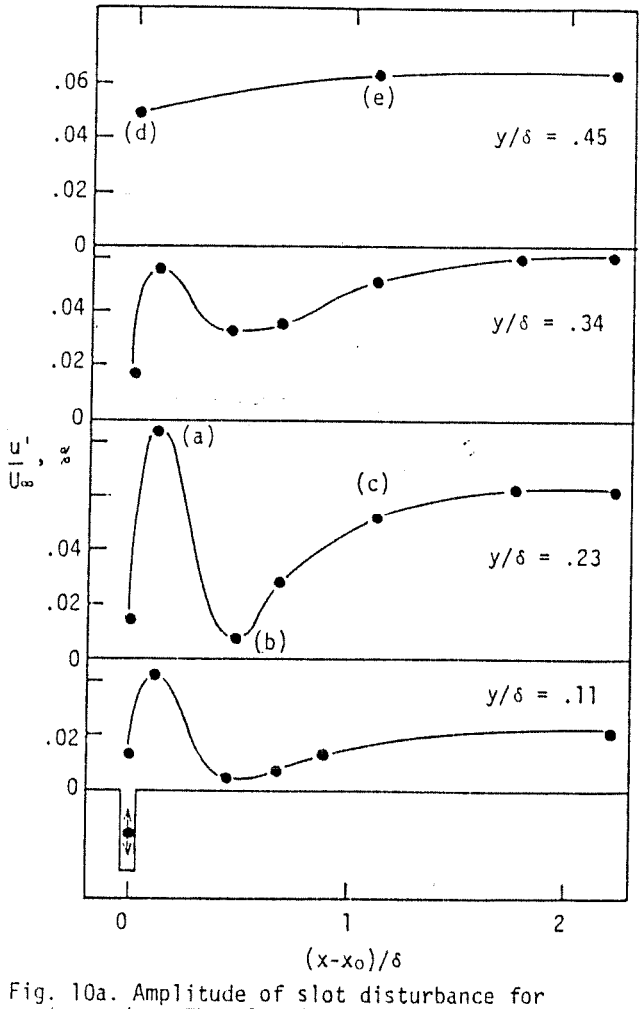

Fig. 10a. Amplitude of slot disturbance for various y/δ. The slot is located at x_o and has a width of approximately $1/15\delta$; U_∞ = 6 m/sec and R_δ^* = 630.

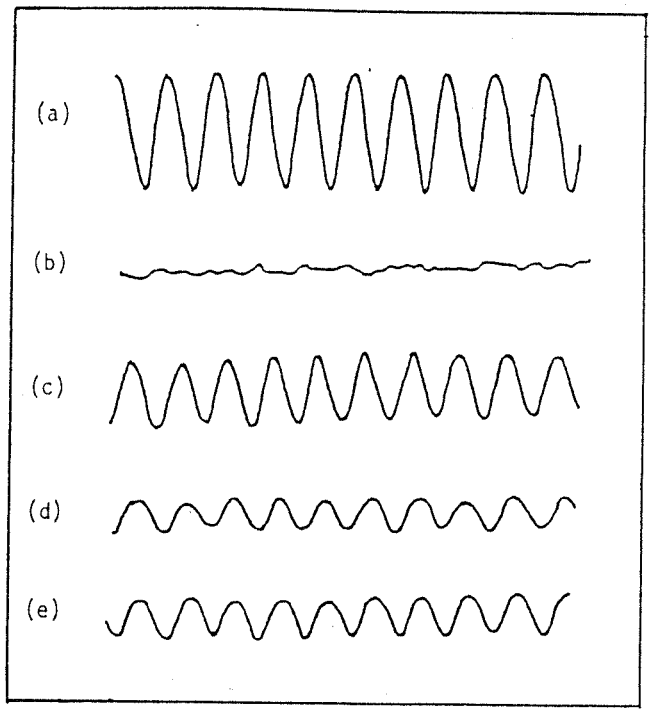

Fig. 10b. Oscillograms recorded at the locations shown in figure 10a.

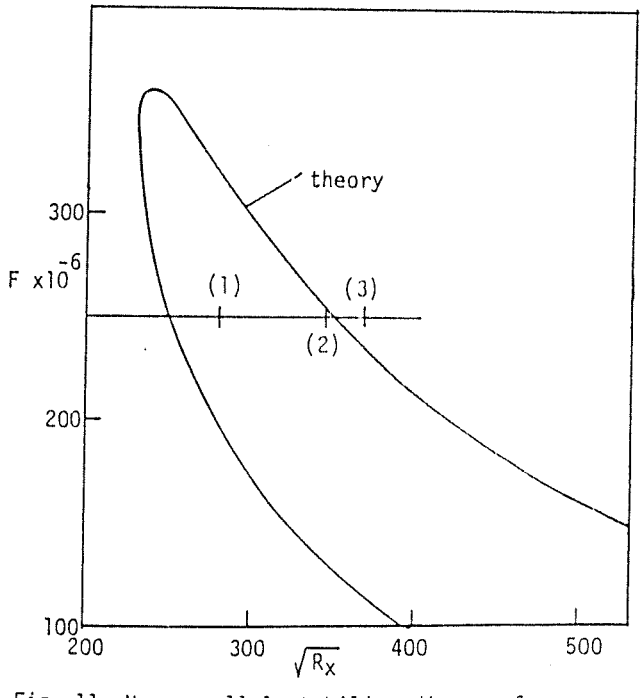

Fig. 11. Non-parallel stability diagram for a zero pressure gradient flat plate boundary layer. At station (1) a controlled T-S wave is produced. A second T-S wave is generated at (2) and all signals were monitored at (3) and downstream; $F = 250 \times 10^{-6}$ where $F = 2\pi f\upsilon/U_\infty^2$.

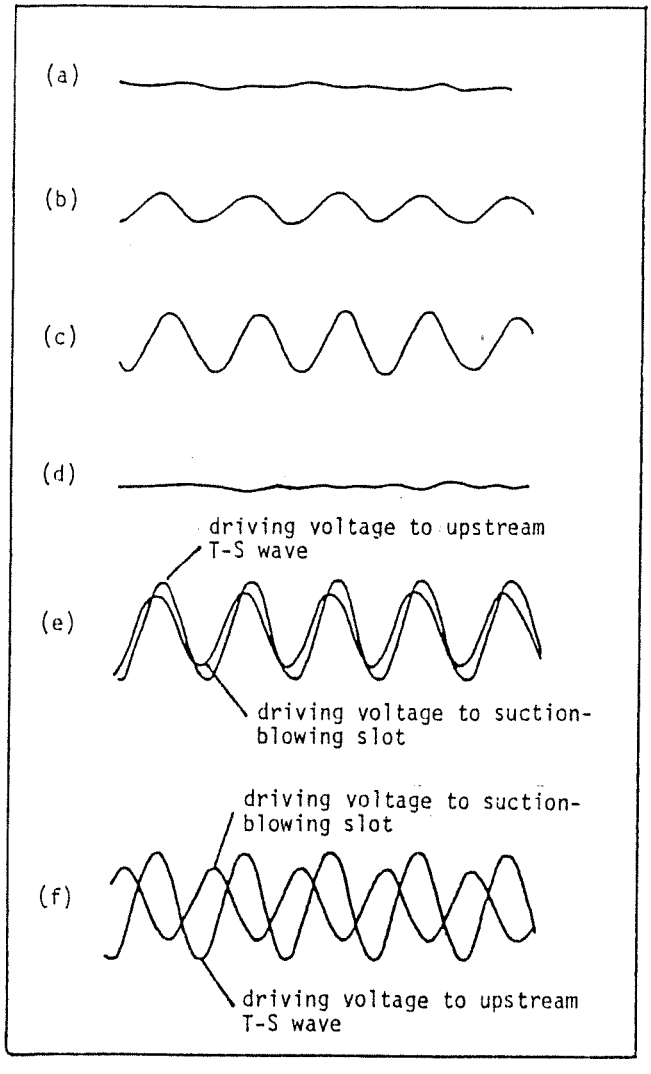

Fig. 12. Oscillograms showing reinforcement and cancellation of a controlled T-S wave by the suction-blowing technique. (a) background disturbances, (b) generated T-S wave, (c) reinforced T-S wave, (d) cancelled T-S wave. Traces (d) and (e) show the driving voltage signals used to produce reinforcement and cancellation respectively.

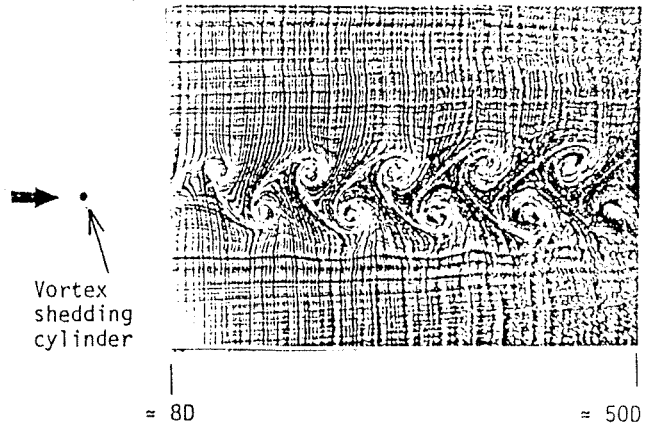

Fig. 13. Hydrogen bubble picture of vortex shedding behind a circular cylinder. Re ≈ 80.

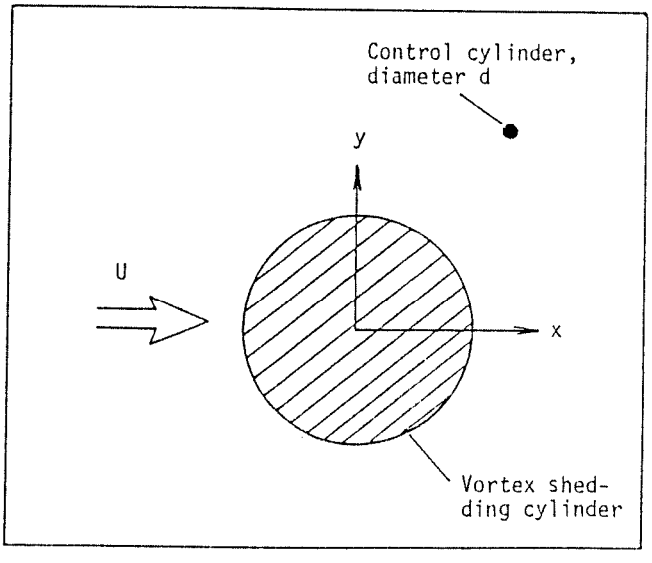

Fig. 14. Schematic of the arrangement for complete control. $D/d \leq 20$.

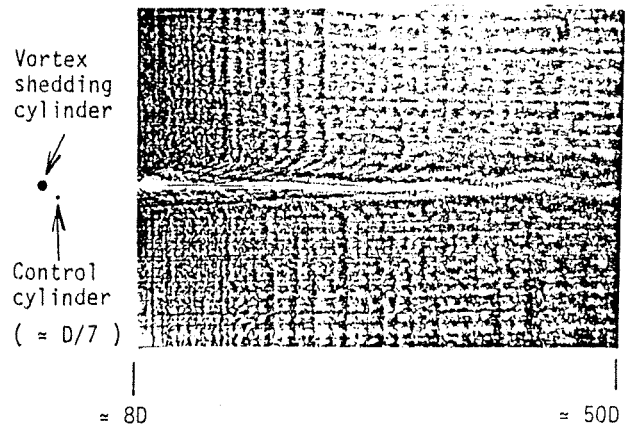

Fig. 15a. The suppression of vortex shedding. The appearance of large scale instability towards the right end of the photograph is unrelated to the Karman vortex street. Re ≈ 80.

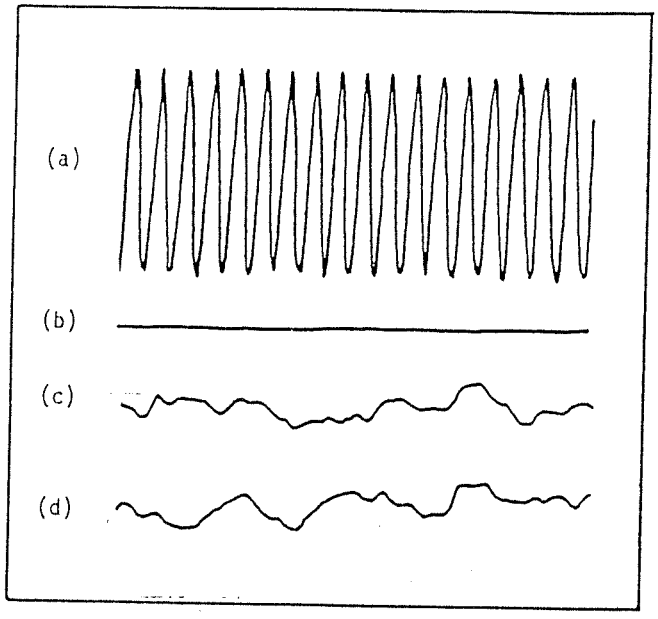

Fig. 15b. Oscillograms in the wake with and without control, Re=71. (a) x/D = 10, about 1D off-axis, no control; (b) x/D = 10, about 1D off-axis, with control, D/d = 11; (c) same as (b), except for an amplification of about 20. (d) x/D = 100, all other conditions same as in (c).

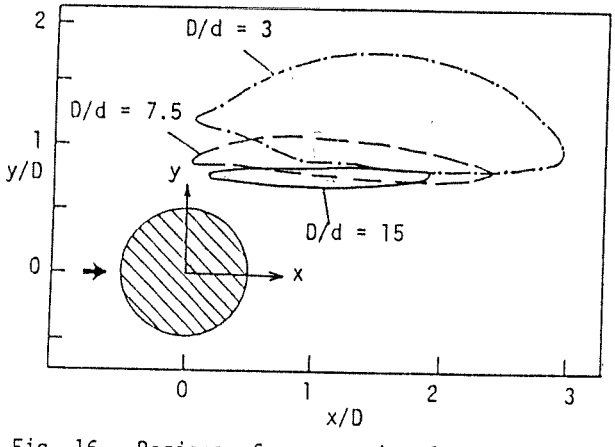

Fig. 16. Regions of suppression for three values of D/d. These regions are symmetrical about the plane y = 0. Re = 80.

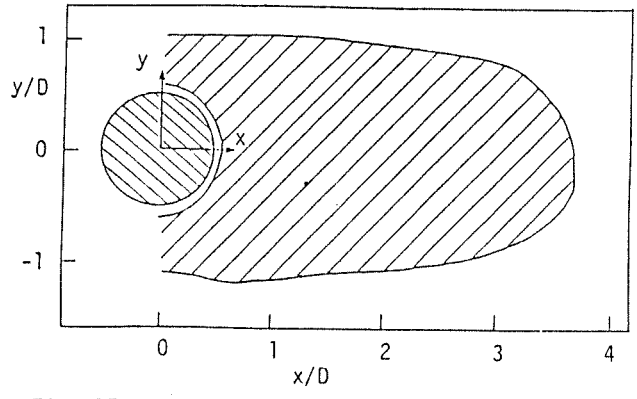

Fig. 17. Hatched area behind the cylinder represents region of suppression when the nichrome control wire is heated (0.5 watt/cm); Re = 80 and D/d = 15.

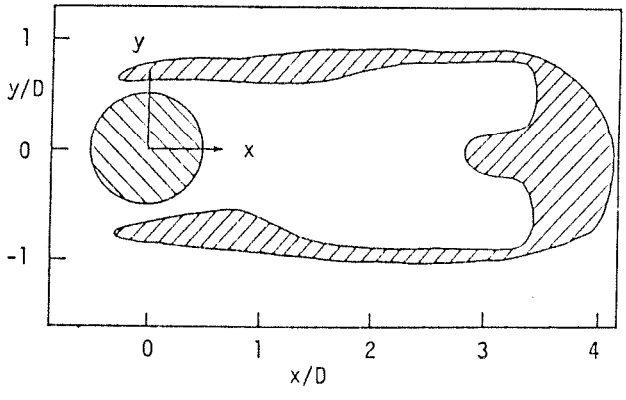

Fig. 18. Hatched area in the wake represents region of suppression at Re = 120 when the nichrome control wire is heated (0.5 watts/cm); D/d = 15.

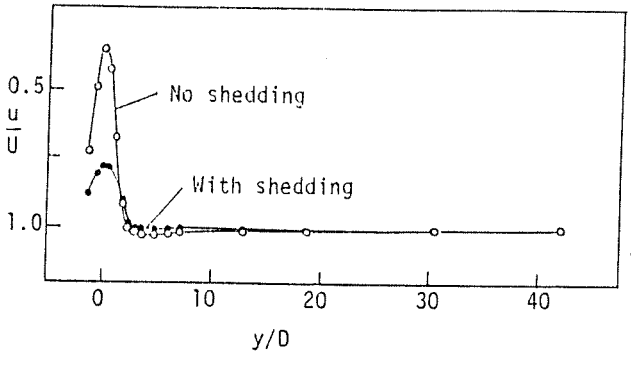

Fig. 19. Mean velocity distribution at x/D = 58, D/d = 8.5 and Re = 65. Notice the long tail for the case with suppressed shedding.

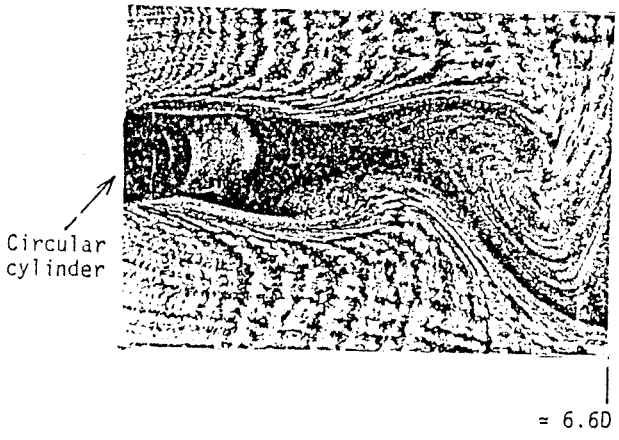

Fig. 20. Details in the near field of the vortex shedding cylinder. Re ≈ 90. No control is applied.

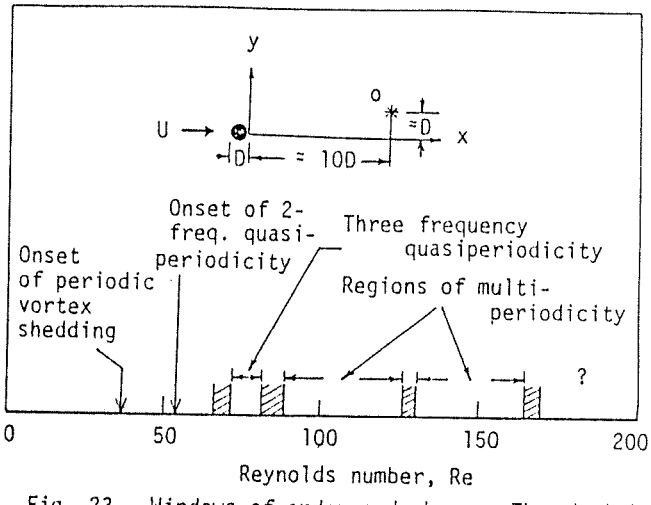

Fig. 23. Windows of order and chaos. The shaded regions correspond to windows of chaos; the in-between regions are regions of quasiperiodicities.

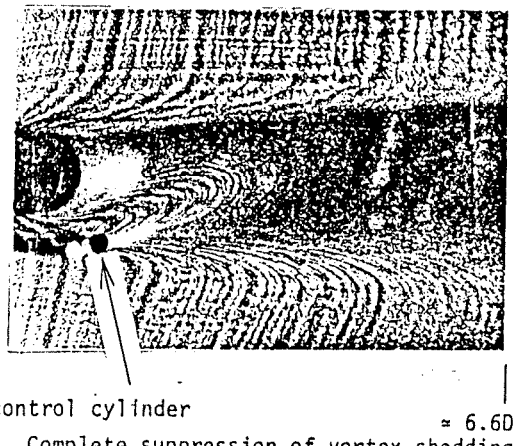

Fig. 21. Complete suppression of vortex shedding; Re ≈ 90, D/d ≈ 7.

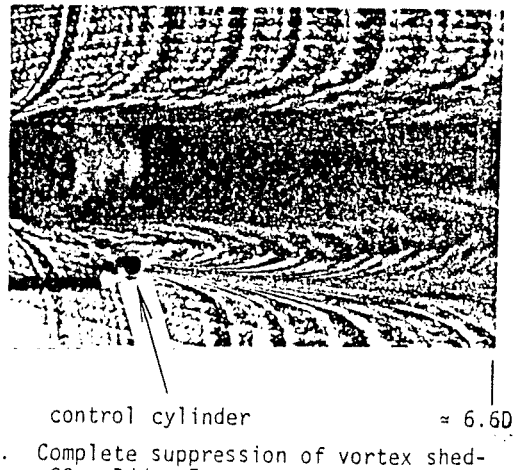

Fig. 22. Complete suppression of vortex shedding; Re ≈ 90, D/d ≈ 7.

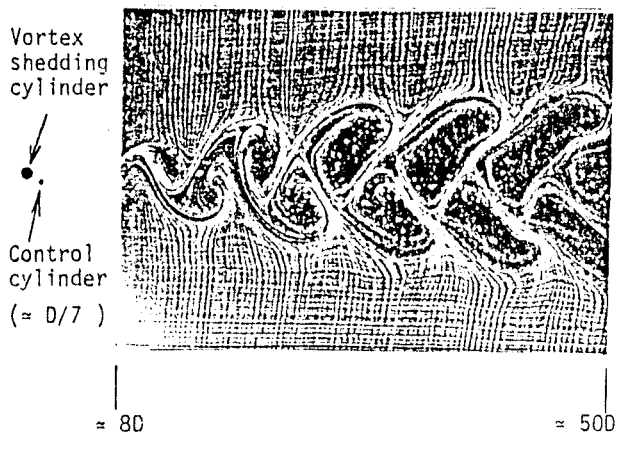

Fig. 24. Modification of the vortex shedding by a suitable placement of the control cylinder; Re ≈ 90.